



HAL
open science

Estimating single molecule conductance from spontaneous evolution of a molecular contact

M. Gil, T. Malinowski, M. Iazykov, Hubert Klein

► **To cite this version:**

M. Gil, T. Malinowski, M. Iazykov, Hubert Klein. Estimating single molecule conductance from spontaneous evolution of a molecular contact. *Journal of Applied Physics*, 2018, 123 (10), 10.1063/1.5018252 . hal-01586755v2

HAL Id: hal-01586755

<https://amu.hal.science/hal-01586755v2>

Submitted on 28 Mar 2018

HAL is a multi-disciplinary open access archive for the deposit and dissemination of scientific research documents, whether they are published or not. The documents may come from teaching and research institutions in France or abroad, or from public or private research centers.

L'archive ouverte pluridisciplinaire **HAL**, est destinée au dépôt et à la diffusion de documents scientifiques de niveau recherche, publiés ou non, émanant des établissements d'enseignement et de recherche français ou étrangers, des laboratoires publics ou privés.

Estimating single molecule conductance from spontaneous evolution of a molecular contact

M Gil, T Malinowski, M Iazykov and H R Klein
CINaM UMR CNRS 7325, Aix Marseille Univ, F-13288, Marseille cedex 9, France

Abstract

We present an original method to estimate the conductivity of a single molecule anchored to nanometric-sized metallic electrodes, using a Mechanically Controlled Break Junction (MCBJ) operated at room temperature in liquid. We record the conductance through the metal / molecules / metal nanocontact while keeping the metallic electrodes at a fixed distance. Taking advantage of thermal diffusion and electromigration, we let the contact naturally explore the more stable configurations around a chosen conductance value. The conductance of a single molecule is estimated from a statistical analysis of raw conductance and conductance standard deviation data for molecular contacts containing up to 14 molecules. The single molecule conductance values are interpreted as time-averaged conductance of an ensemble of conformers at thermal equilibrium.

1 Introduction

Molecular electronics (i.e. electronic components based on a single molecule [1] or a molecular assembly) as been the focus of extensive research for more than a decade. However, despite the wide range of problems addressed, a basic question remains : what can we learn from the conductance of a single molecule, and what are the main factors that affect the magnitude of measured conductances [2]?

Of the techniques used to study electrical conduction through molecules [3], Scanning Tunneling Microscopy (STM [4]) and Break Junction techniques [5] are the most appropriate ways to measure electrical conduction through a single molecule [6, 7]. These two techniques make use of nanometric- or atomic-sized electrodes [8] to connect a single molecule and measure the current flowing through it. Despite the simplicity and unicity of the principle, the results obtained often exhibit a large spread (see e.g. figure 15 of ref. [3]), since single molecule conductance strongly depends on experimental conditions [9].

STM in break junction mode (STM-BJ) is probably the easiest and the most widely used technique when dealing with single molecule conductance [10]. In an STM-BJ set-up, metallic junctions are repeatedly formed by indenting a metallic surface with a tip, and broken by stretching the contact, leading to nanometric-sized metallic electrodes. Working in an organic solution, properly functionalized molecules can spontaneously bond to the electrodes, making it possible to measure the conductance of these molecular bridges. In these experiments , however, the molecular junction is continuously stretched during

measurements. This stretching induces a strain which reduces the lifetime of the junctions [11, 12, 13], influencing the conformation of the molecules within the contact, and thus their conductance (see e.g. [14, 15]). This can be viewed as a drawback and makes it difficult to analyze conductance data [16]. Moreover, in these molecular junctions, current is flowing through different parallel paths : the molecule(s) and a tunneling channel. When the distance between electrodes varies, the contribution of each path to the total conductance evolves, making it difficult to analyze conductance data. This has necessitated the development of dedicated analysis procedures [17, 18].

An alternative measurement technique has been proposed by W. Haiss and co-workers using an STM [19]. This method consists in trapping molecules between an STM tip and a surface kept at a constant distance. The molecules, upon thermal motion, spontaneously connect (disconnect) the two electrodes. Abrupt jumps in the tunneling current are clearly observed, attributed to molecular connection events, and single molecule conductance values are extracted unambiguously. This technique provides further insights into the conduction mechanism at the single molecule scale [20]. It highlights the temperature dependence of molecular conductance, governed by the conformer distribution of the molecules.

The present work reports an original technique, using a Mechanically Controlled Break Junction (MCBJ), and derived from the above technique. The key idea is to take advantage of thermal diffusion and electromigration at room temperature to let the contact self-organize at the atomic scale, so that it naturally explores the more stable configurations around an average chosen conductance value. Similar “random” approaches have successfully been applied to extract information from disordered or stochastic systems [21, 22]. At the nanometric scale, tracking of diffusion processes gives rise to stochastic signals often in the form of random telegraphic signals . Unbiased statistical analysis of these signals can provide access to valuable information [23, 24] without requiring underlying assumptions.

In the case of a molecular contact containing several molecules bridging two metallic electrodes, current is likely to vary in response to connection / disconnection events. If the contact contains only one type of molecule, all the individual events may be of the same amplitude, irrespective of the number of molecules forming the contact. In this situation, the conductance of a single molecule should be extracted from an analysis of these events. It should be noted that this quantity represents the conductance of a single molecule anchored to its metallic electrodes, thus including the intrinsic molecular conductance and the conductance of the contacts [29].

In the following, we present our experimental set-up and measurement principle. We fix the distance between the two metallic electrodes of the MCBJ and record the temporal evolution of the current flowing through it. Analyzing measurements performed on widely studied molecules, alkanedithiols, we show the pertinence and promise of this measurement technique by estimating the conductance of a single molecule from the spontaneous (thermal) evolution of molecular contacts composed of up to 14 molecules.

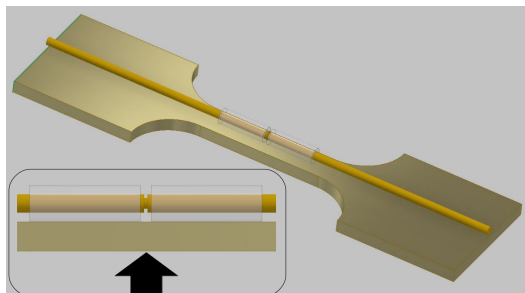


Figure 1: Schematic of the sample used for our MCBJ. The samples are made from Au wire glued into two quartz capillaries which are then glued onto a phosphorous bronze bending beam. As seen in the inset, the wire is notched in the empty space between the capillaries to initiate the breaking of the junction. See text for more details.

2 Methods

2.1 Experimental setup

Our set-up consists of a home-made MCBJ (described in [13]), and the related acquisition and control electronics and informatics. The MCBJ was first introduced by Muller [5], based on an earlier design by Moreland and Ekin [25]. The basic principle consists in stretching a metallic wire by bending an elastic substrate supporting the wire with a mechanical actuator until the junction breaks, giving two separate electrodes. The electrode separation can then be adjusted by a feedback loop using the current flowing through the junction. MCBJ exhibits excellent mechanical stability, which results from the reduction of the mechanical loop connecting one electrode to the other. For this study, our MCBJ is operated at room temperature in organic solutions.

Figure 1 represents a sample for our MCBJ. They are made from Au wire (250 μm diameter, 99.99%, Goodfellow) glued into two quartz capillaries (fused silica, 1mm inner diameter, Vitrocom) which are then glued onto a phosphorous bronze bending beam. An optical glue (NOA61, Nordland) is used for both bondings. The wire is notched in the empty space between the capillaries to initiate the breaking of the junction. The free-standing part of the Au wire is typically 200 μm for our samples, and the unfilled parts of the capillaries act as a reservoir for the organic solutions. Before use, samples are cleaned in a plasma cleaner (ATTO, Diener Electronic) operated with an air pressure of 0.4 mbar at a power of 30W for two minutes.

The separation of the electrodes is controlled by a micrometer step motor (Z-825, Thorlabs) stacked-up with a piezoelectric actuator (sensitivity : 216 nm.V^{-1}). Motor and piezo are driven through an input/output board by a dedicated computer interface, which is also used for acquiring data and feedbacking. Because the wire is fixed, the actuator motion is demagnified, allowing accurate control of wire stretching. Taking into account a typical push:stretch ratio of 20:1 and the resolution of our 16-bit DAC, one digit corresponds to less than 3 pm , which is ample for this work. As the stability of the MCBJ is a

critical parameter for this study, it is operated in the basement of the laboratory on an optical table to ensure optimal isolation from mechanical vibrations in a temperature-controlled environment (temperature variations below 1°C on a 24 hour scale). At low bias (typically, $V_{bias} \simeq 130\text{ mV}$ for this study) and at room temperature, the drift of the electrodes is below $5\text{ pm}\cdot\text{s}^{-1}$ after one or two hours of operation.

The conductance is derived from the intensity that flows through the junction, measured using a home-made current/voltage converter with a logarithmic trans-conductance gain following the design proposed by U. Dürig [26]. This converter allows measurements from the 100pA range (noise level of 10pA on a 10 kHz bandwidth) up to the mA range, and is operated at a constant temperature of 20°C . Prior to measurements, the converter is carefully calibrated with a series of precision resistors ($1, 10, 100\text{ M}\Omega$ and $1\text{ G}\Omega$ 0.1% resistors from Caddock). These calibration data are then used to calculate the current or conductance values corresponding to the output voltage. The junction, in series with a $1\text{ k}\Omega$ ballast resistor to avoid saturation of the transimpedance amplifier, is biased using a 6V lead battery. The voltage output of the transimpedance amplifier is recorded using a 16-bit ADC, operated at a sampling frequency of 32768 Hz . Fresh millimolar solutions of alkanedithiols (octanedithiols ODT $\geq 97\%$, and pentanedithiol PDT 96% , Aldrich) in mesitylene (98% , Aldrich) are prepared and immediately used for measurements.

2.2 Measurement and analysis protocol

To ensure cleanliness of the contacts, samples are broken in pure solvent (mesitylene). They are operated for one or two hours at a typical setpoint of 200 pA before measurements begin, to allow mechanical relaxation of the bending beam, and thus stabilization of the electrode distance. When certain that we observe no noticeable current drift (beyond the noise level of the converter) on a minute range, we begin the measurements.

We feed the sample with $10\text{ }\mu\text{L}$ of solution and set a current setpoint in the sub nA range. This current imposes the distance between the gold electrodes, and after stabilization, the feedback loop controlling the electrode separation is disabled.

We then observe the temporal evolution of the current flowing through the contact. A connection or disconnection of a molecule between the 2 electrodes is expected to induce a sharp change (stepwise) in the current. If we do not observe such events, the feedback is enabled, and the setpoint is increased (reducing electrode separation). These operations are repeated until we observe abrupt current jumps.

Taking advantage of thermal diffusion and electromigration, at room temperature, the nano-contact self-organizes at atomic level and naturally explores the more stable configurations around the average chosen conductance value. During these periods we record the temporal evolution of the current flowing through the contact. We operate the piezo actuator only if the current falls below 20 pA or rise above 10 nA . The recording of the current is interrupted when the piezo actuator is active.

Figure 2 illustrates a 10 s recording of the current flowing through a junction filled with an octanedithiol solution and operated at a bias voltage of 139 mV . A random telegraphic signal is clearly observed, corresponding to numerous

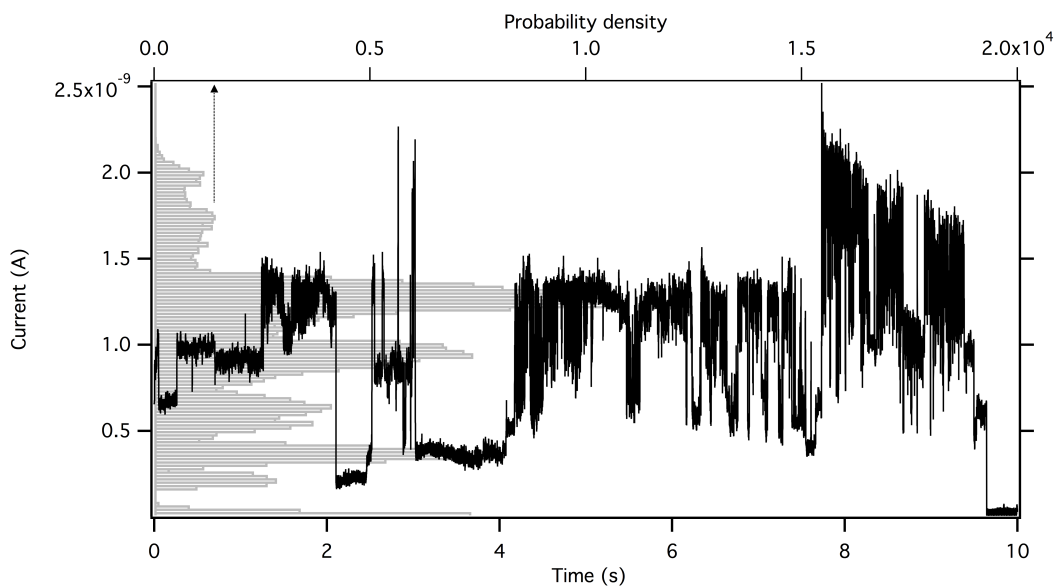


Figure 2: Spontaneous evolution of the current of a molecular contact formed from a millimolar octanedithiol (ODT) solution in mesitylene. Prior to recording, the junction is operated for 2 hours in pure solvent. The recording starts 5 minutes after the junction is refilled with the ODT solution. The electrode separation is fixed with a setpoint current of 0.5nA before the regulation feedback is disabled (see text for more details). Current (black continuous line) is recorded, and a bias of 139mV is applied to the junction. A histogram of the current (gray) clearly indicates the most probable current values.

molecule connection / disconnection events in the contact. A histogram of the current also clearly illustrates the discrete nature of current jumps and the most likely values of the current. This histogram and the others presented below are all constructed using the rule suggested by D.P. Doane [27] for data binning, in order to be able to compare histograms constructed from datasets of different sizes¹.

From the temporal evolution of the current (or conductance in the following) we can construct the distribution of the time spent in a given state by calculating the time lags between consecutive current jumps. Jumps are located by tracking variations in current standard deviation with a rolling window of 10 data points (equivalent to a cutoff of 0.3 ms for a sampling rate of 32768 Hz). We define a jump as a variation of more than 5 times the median standard deviation value of the current recording.

3 Results

Our main objective being to present the measurement technique, we conducted this work on widely studied saturated model molecules, alkanedithiols. We chose two alkanedithiol chains of different lengths : octane- and pentane- dithiols containing respectively 8 and 5 carbon atoms in their saturated backbones. These molecules bind to metallic electrodes via their terminal thiol groups. Previous studies have shown unambiguously that transport through alkanedithiols can be approximated by a non-resonant tunnelling process through a barrier whose width is determined by the distance between the terminal groups of the molecule [19]. We thus expect a higher conductance for the shorter pentanedithiol molecule than for the longer octanedithiol molecule, considering that both molecules have similar contact conductances.

In figure 3 (right), we compare conductance recordings for PDT and ODT millimolar solutions in mesitylene, with a bias voltage of 139mV, and setpoint currents of respectively 0.2nA and 0.6nA for ODT and PDT. As explained above, these setpoints were chosen as the smallest setpoints where we observe current jumps. A higher setpoint means that electrode separation is smaller for PDT, which is in agreement with the fact that PDT molecules are shorter than ODT molecules. Both histograms exhibit similar features : a series of evenly spaced peaks in conductance. The measurements realized in pure mesitylene do not exhibit such features, with the exception of current fluctuations around the selected current setpoint (0.2 nA for a bias voltage of 0,139V, $G = 1,9.10^{-5}G_0$), as seen on figure 3(left).

Figure 4 (left) shows the conductance values corresponding to the clear peaks of both histograms of figure 3 on a graph where the abscissa is a number of molecules. The lowest conductance value is arbitrarily attributed to one molecule. The graph clearly shows that conductance values are fitted by a linear function $f(N_{MOL}) = G_{MOL}.N_{MOL}$, G_{MOL} being the conductance of a single molecule, and N_{MOL} the number of molecules. From linear fits of these data points we extract two G_{MOL} values : $G_{PDT} = 1.22.10^{-5} \pm 5.10^{-7}G_0$ for PDT, and $G_{ODT} = 6.7.10^{-6} \pm 4.10^{-7}G_0$ for ODT.

Experiments were repeated for different setpoints for PDT and ODT. We do not expect strong dependence of the single molecule conductance on the

¹Current recordings typically contain from 10^7 to 10^8 samples.

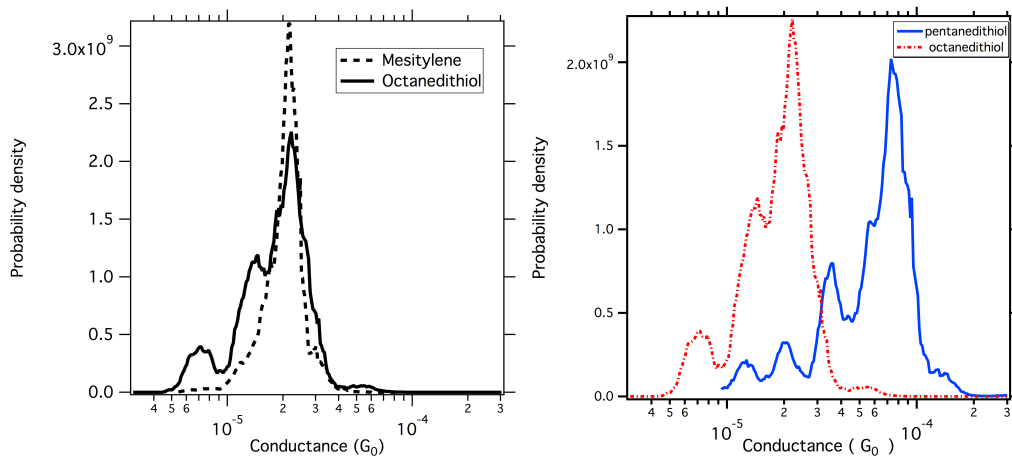


Figure 3: **Left** : Comparison of conductance histograms for a junction operated in pure mesitylene (black dashed line) and in a millimolar solution of ODT in mesitylene (black continuous line). Bias voltage : 139 mV, setpoint current used to fix the electrode separation : 0.2nA. While the solvent's histogram does not exhibit particular features apart from random fluctuations around the setpoint current, it can be seen that a junction containing ODT molecules explores more conductance values and exhibits peaks representing the most probable conductance values. **Right** : Comparison of conductance histograms for a junction immersed in octane (online version red) and pentanedithiols (online version blue). Bias voltage : 139 mV, setpoint current 0.2nA for octanedithiols and 0.6nA for pentanedithiols. Each histogram exhibits similar features : series of evenly spaced peaks in conductance, which we attribute to the discrete variations in conductance related to the number of molecules in the contact.

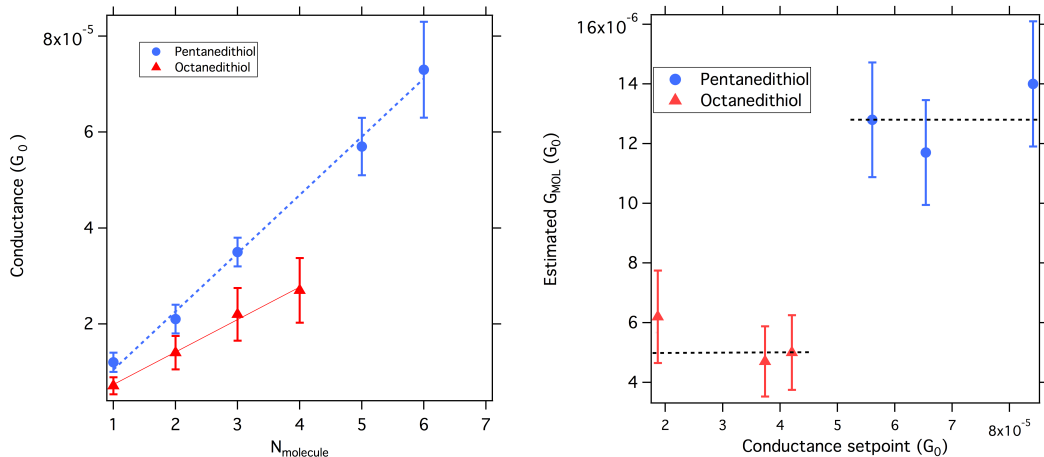


Figure 4: **Left** : Conductance values of the peaks for the histograms of figure 3 versus a number of molecules. The lower values are attributed to a single molecule as we do not observe current jumps of lower amplitude. A linear fit of these curves gives a conductance per molecule of $G_{PDT} = 1.22 \cdot 10^{-5} \pm 5 \cdot 10^{-7} G_0$ for PDT, and $G_{ODT} = 6.7 \cdot 10^{-6} \pm 4 \cdot 10^{-7} G_0$ for ODT. **Right** : Estimation of conductance values for a single molecule for different conductance setpoints. Bias voltage : 139 mV. The estimated molecular conductance does not depend on the chosen setpoint current.

chosen setpoint; the setpoint only fixes the initial configuration of the contact, and thus the number of molecules initially present. This is shown on figure 4(right), where we plot 3 values of G_{MOL} obtained from experiments following the same protocol at different setpoints for both PDT and ODT. These values are identical.

The discrete variations in conductance allow us to estimate single molecule conductance from a statistical analysis of raw conductance recordings. However, this evolution is rapidly smeared out by conductance fluctuations. It is therefore worth investigating whether current fluctuations can also provide information concerning the discrete evolution of the contact. If we make the assumption that the conductance fluctuation amplitude is related to the number of molecules acting as noise sources in the contacts, a discrete variation is expected.

To further explore these variations in conductance we estimate these fluctuations by calculating the standard deviation of the conductance of the contacts, integrated over the bandwidth of our recording set-up. Although it is not designed for accurate noise measurements, it still gives us interesting information. Directly plotting the conductance standard deviation vs the conductance gives an informationless cloud of points. We applied to these data a binning procedure successfully used for another study [22]. We divide standard deviation data in classes over the conductance axis, using Doane's rule. We then calculate the median standard deviation value for each class. The result of this analysis for the PDT and ODT experiments of figure 3 is shown in figure 5. We can see a constant increase in standard deviation as the conductance increases. Despite the rough estimation method used, beyond the noise floor of our setup (stan-

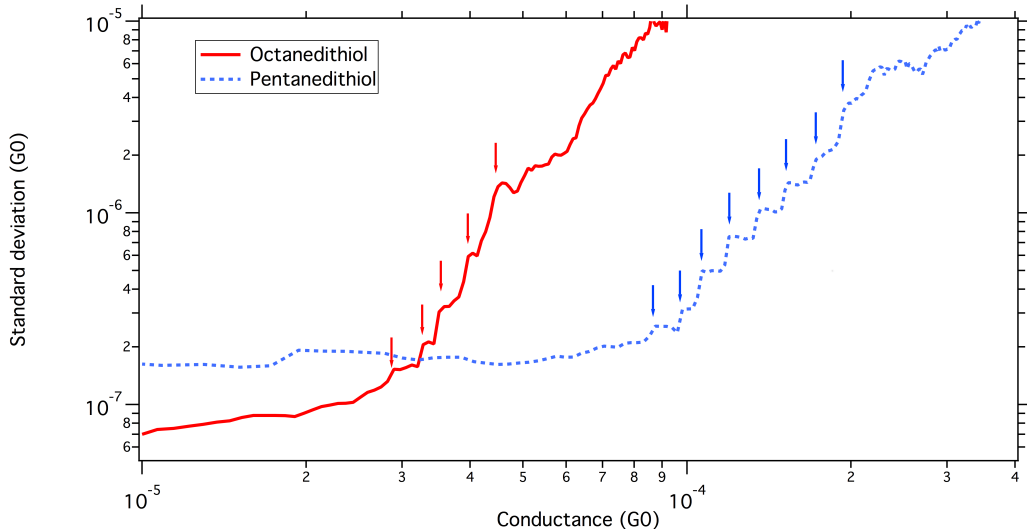


Figure 5: Conductance standard deviation calculated for ODT (continuous line) and PDT (dashed line). Standard deviation data have been binned along the conductance axis (see text for details), and median value of the standard deviation has been calculated for each bin. For both molecules, jumps in the standard deviation appear clearly. The spacing between the jumps along the conductance axis is equal to individual conductance.

dard deviation larger than $10^{-7}G_0$), jumps in standard deviation occur for a limited range of conductance : $3 - 5 \cdot 10^{-5}G_0$ for ODT and $0.9 - 3 \cdot 10^{-4}G_0$ for PDT. It is noteworthy that these jumps occur at evenly spaced conductance increases. Moreover, these values are consistent with those extracted from conductance histograms of figure 3, but higher. Interestingly, when conductance jumps are smeared out by fluctuations, the discrete nature of the molecular contacts is still visible in the fluctuations, although in a limited range. It allows us to perform a statistical analysis of the conductance of the contact on a larger set of observations; this is discussed in the next section.

4 Discussion

The key idea behind this work is to estimate the conductance of individual molecules anchored to metallic electrodes when no external mechanical strain is applied. This is achieved by observing, in an MCBJ, the spontaneous evolution of a molecular contact formed between two metallic electrodes kept at a fixed distance, through the evolution of conductance.

In this situation, the reconfiguration of the molecular contact is thermally driven (see e.g.[24]). Many processes can alter the conductance of the contact : connection or disconnection of molecules, atomic rearrangements of the metallic electrodes and structural changes in the molecules. Rearrangements of electrodes [28], and molecular conformational changes [31], are expected to occur at a time scale below the nanosecond, which means that only averaged values will

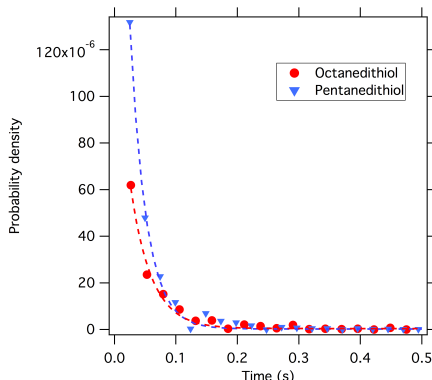


Figure 6: Histogram of the time lag separating conductance jumps for pentane and octanedithiol in mesitylene. The mean time can be interpreted as the lifetime of one molecule in the contact. A fit (lines on plot) with an exponential function $A \cdot \exp(-t/\tau)$ gives equivalent times $\tau_{PDT} = 2.6 \cdot 10^{-2} \pm 5.1 \cdot 10^{-3}$ s for PDT, and $\tau_{ODT} = 3.4 \cdot 10^{-2} \pm 1.3 \cdot 10^{-2}$ s for ODT.

be measured within the limited bandwidth of our set-up. However, molecular connection in the contact is expected to occur at a millisecond time scale, given the chemical affinity of the thiol group to the gold electrodes [32].

From the temporal analysis of current jumps shown in figure 6, we estimate mean time constants for connection / disconnection of molecules to be 30ms for both PDT and ODT. The mean lifetimes of connection events for the two studied molecules are very similar, since they are very similar and share the same anchoring group.

We can thus state that these events are responsible for the abrupt current jumps that we systematically observe in molecular contacts. The current flowing through the electrodes comes from two channels : a tunneling channel whose conductance depends mainly on the electrode separation, and a molecular channel whose conductance depends on the nature, the number and possibly the conformation of the molecules. With a constant distance between electrodes, the contribution of the tunneling channel does not vary, or only slowly due to thermal drift of the set-up.

By building a conductance histogram from current recording during the evolution of a contact, we obtain peaks indicating the most probable values. In our situation, these values should correspond to integer numbers of molecules within the contact, and are therefore expected to share a smallest common multiple, which we assign to the conductance of a single molecule. One of the main benefits of such an analysis lies in eliminating the constant (or slowly varying) tunneling contribution to net conductance, provided that several conductance values corresponding to different contact configurations are measured.

Thanks to the outstanding mechanical stability of our setup, we estimate the conductance of a single molecule to be $G_{PDT} = 1.28 \cdot 10^{-5} \pm 0.21 \cdot 10^{-5} G_0$ for PDT, and $G_{ODT} = 5.3 \cdot 10^{-6} \pm 1.1 \cdot 10^{-6} G_0$ for ODT. These values are in quantitative agreement with values published for PDT and ODT, using a similar approach [19]. The fact that at least 5 evenly spaced conductance peaks are

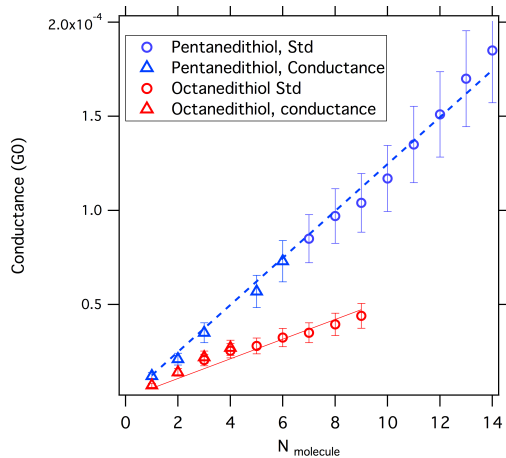


Figure 7: Conductance values corresponding to a discrete number of molecules in PDT and ODT contacts. The plot gathers data extracted from figure 4(left) and 5. It shows that the conductance values extracted from the two analyses are in excellent agreement. From linear fits we estimate the conductance of a single molecule to be $G_{PDT} = 1.25 \cdot 10^{-5} \pm 0.19 \cdot 10^{-5} G_0$ for PDT and $G_{ODT} = 5.27 \cdot 10^{-6} \pm 0.22 \cdot 10^{-6} G_0$ for ODT.

observed in the conductance histograms is a clear indication that the position of the electrodes remains fixed throughout the recording (typically 10 seconds to one minute). It is noteworthy that we found values within the confidence intervals for both molecules (data not shown) at different biases (260 and 420 mV). Within this bias range, there is likely to be no resonance with molecular levels of the alkanedithiols, and therefore a constant conductance value is expected.

The histograms in figure 3 exhibit peaks for up to 6 molecules in the contact. At higher conductances, fluctuations smear out the current jumps and peaks are difficult to assign in the histogram representation. A further step is to analyze the conductance fluctuations. If we make the reasonable assumption that the conductance fluctuations in the contact depend on the number of molecules, jumps in the fluctuations should be observed when the number of molecules varies. Moreover these jumps should be evenly spaced in conductance, like the peaks in the conductance histograms. This is the main feature of figure 5, where the arrows indicate these conductance fluctuation jumps which, as expected, are evenly spaced in conductance.

Figure 7 is a plot gathering conductance values corresponding to the discrete number of molecules for PDT and ODT, from conductance and standard deviation analysis. It shows an excellent agreement for conductance values extracted by both methods. From it, we more robustly estimate the conductance of a single molecule to be $G_{PDT} = 1.25 \cdot 10^{-5} \pm 0.19 \cdot 10^{-5} G_0$ for PDT, and $G_{ODT} = 5.27 \cdot 10^{-6} \pm 0.22 \cdot 10^{-6} G_0$ for ODT, from the spontaneous evolution of molecular contacts containing up to 9 molecules for ODT, and 14 for PDT. To our knowledge, the literature offers no analysis constructed from raw data.

The conductance values, while in quantitative agreement with those previously obtained from spontaneous molecular connections [19, 20], are lower than

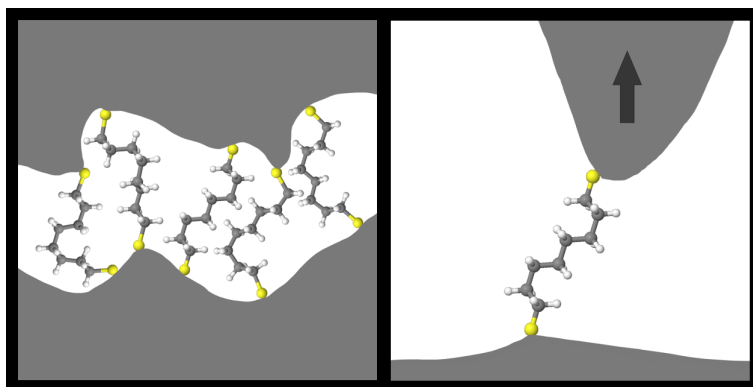


Figure 8: Schematic illustration of conductance measurements in an MCBJ (left) and a STM-BJ (right) setup. While the traction of the anchored molecule by the STM tip favors the *all-trans* conformers of alkanedithiol molecules in STM-BJ measurements, the morphology of the MCBJ electrodes allows the coexistence of multiple conformers of the molecules

those generally extracted from STM-BJ experiments on alkanedithiols (see e.g. [33, 14]). This can be attributed to the superpositioning of a tunneling channel onto the molecular channel in STM-BJ experiments, making it tricky to compare absolute conductance values. If instead we compare conductance ratios for PDT and ODT, we obtain a ratio $G_{PDT}/G_{ODT} = 2.37 \pm 0.46$ in our experiments, in disagreement with the conductance ratio of 20 ± 6.1 reported in the the pioneering work of N.J. Tao and co-workers [10].

Conductance measurements are finely modeled with a simple tunneling model for saturated molecules such as alkanedithiols, and the conductance is expressed as $G \simeq \exp(-\beta \cdot N)$, with β a decay constant expressed per carbon atom in the molecular backbone, and a prefactor taking into account the contact resistance (estimated to 6 k Ω for alkanedithiols anchored to gold electrodes [30]). A value of $\beta = 1.0 \pm 0.1$ is often reported leading to the conductance ratio of 20 ± 6.1 in [10].

We now discuss this apparent discrepancy, which we attribute to the fact that the conductance values reported here represent an averaging over a conformer population at thermal equilibrium of the same molecule.

Alkane molecules present different conformers from *all-trans* (conformer of lower energy) to *all-gauche* con-formations (conformer of higher energy). At thermal equilibrium, the fractional population of different conformers follows a Boltzmann's distribution. For alkanes in general, the activation energy for conformer interconversion (corresponding to the rotation of a methyl group around a carbon-carbon bond) is about 14kJ.mol⁻¹ (0.15 eV per molecule). When measuring the conductance of a molecule at room temperature and at a millisecond time scale following our protocol, the conductance is therefore a time average of an ensemble of conformers.

The PDT molecule presents 4 conformers, from the *all-trans*, with the largest distance between terminal groups, to the most folded conformer with the smallest. The length difference between the terminal groups for these two conformers

is $\Delta d = 0.15\text{nm}$. If we make the simplest approximation that, for different alkanedithiols or different conformers of the same alkanedithiol, the barrier medium is the same, and its width is related to the distance between terminal groups, the *all-trans* conformer has the largest barrier, while the *all-gauche* has the smallest. If we calculate a tunneling current through a one-dimensional rectangular barrier described by the decay constant κ in nm^{-1}

$$\kappa = \left(\frac{2m_e^*\phi}{(\hbar/2\pi)^2} \right)^{1/2} \quad (1)$$

where \hbar is the Planck's constant, ϕ the barrier height (in J) and m_e^* the effective electron mass, taking $\phi = 5\text{eV}$ and m_e^* as the rest mass of the electron, we obtain for PDT a conductance ratio from the shortest to the longest conformer of 40. Tunneling through the minimum energy configuration (i.e. all trans conformer) is unfavorable compared to higher energy conformations potentially offering higher tunneling probabilities. Therefore, the contribution of each conformer to the measured conductance is not directly proportional to its energy or probability of being occupied.

This has been shown by W. Haiss and co-workers [20], through the experimental and theoretical study of the temperature dependence of single alkanedithiol molecule conductance. The dependence (conductance increases with temperature) is explained, using a simple 1D tunneling barrier, by the change in the distribution between molecular conformers induced by temperature changes. From their results at room temperature, we can calculate a conductance ratio $G_{PDT}/G_{ODT} = 4 \pm 1.3$ in excellent quantitative agreement with our values.

In STM-BJ experiments, molecules are stretched during measurements, as illustrated in figure 8. In these conditions the conformer populations are no longer in thermal equilibrium, and thus, *all-trans* conformers are expected to be favored, leading to a higher G_{PDT}/G_{ODT} ratio. Moreover, the contribution of a parallel tunneling channel in STM-BJ experiments may also increase the discrepancy with our results.

5 Conclusion and Perspectives

We presented an original method to estimate the conductance of a single molecule anchored to metallic electrodes, by measuring the conductance of a molecular contact whose evolution is thermally driven. Spontaneous connections / disconnections of molecules within the contact are evidenced by abrupt conductance jumps at a millisecond time scale. The most probable configurations of the contact lead to conductance values that are linearly spaced. We attribute these values to the opening / closing of conductance channels as a result of discrete variation in the number of molecules in the contact. We estimated the conductance of a single molecule from a statistical analysis of raw conductance recordings on molecular contacts containing up to 14 molecules. While conceptually simple, this experiment relies on the outstanding mechanical stability of our MCBJ set-up, as the distance between the metallic electrodes must be kept constant during the measurements.

We obtained conductance values for two molecules PDT and ODT, using a robust statistical analysis method which removes the tunneling contribution

of the electrodes from the net molecular conductance. In contrast to STM-BJ experiments, we measured the time-averaged conductance of an ensemble of conformers in thermal equilibrium at room temperature.

Discrete variation in conductance and conductance standard deviation is observable for up to 9 molecules in the contact for ODT, and 14 for PDT. If we suppose that the molecules are packed in the contact with a typical distance between sulfur groups of 0.5nm [34], we can estimate the lateral extension of the larger aggregates to be in the range 1.5-3 nm. For larger aggregates, discrete variation in conductance is no longer visible, probably hidden by conductance fluctuations larger than the contribution of a single molecule. While quantitative noise analysis is far beyond the scope of this article, the measurement technique we detailed here opens the way to such studies on nanocontacts of tunable cross section, which are rarely reported [35]. Its use promises new insights into the dynamic and transport mechanisms of nanometric-sized molecular contacts at room temperature.

6 acknowledgments

This work was partially funded by the ANR grant FOST, ANR-12-BS10-01801. We would like to thank Ms M. Sweetko for careful proof reading and English revision, Mr M. Lagaize for technical drawings and Ms T. Klein for artistic drawings.

References

References

- [1] Hyunwook Song, Mark A. Reed, and Takhee Lee. Single molecule electronic devices. *Advanced Materials*, 23(14):1583–1608, 2011.
- [2] A. Salomon, D. Cahen, S. Lindsay, J. Tomfohr, V. B. Engelkes, and C. D. Frisbie. Comparison of electronic transport measurements on organic molecules. *Advanced Materials*, 15(22):1881–1890, 2003.
- [3] H B Akkerman and B de Boer. Electrical conduction through single molecules and self-assembled monolayers. *Journal of Physics: Condensed Matter*, 20(1):013001–, 2008.
- [4] G. Binnig, H. Rohrer, Ch Gerber, and E Weibel. Surface studies by scanning tunneling microscopy. *Phys. Rev. Lett.*, 49(1):57–61, July 1982.
- [5] C. J. Muller, J. M. van Ruitenbeek, and L. J. de Longh. Conductance and supercurrent discontinuities in atomic-scale metallic constrictions of variable width. *Phys. Rev. Lett.*, 69(1):140–143, 1992.
- [6] Fang Chen, Joshua Hihath, Zhifeng Huang, Xiulan Li, and N.J. Tao. Measurement of single-molecule conductance. *Annual Review of Physical Chemistry*, 58(1):535–564, 2007. PMID: 17134372.

- [7] Florian Schwarz and Emanuel Lörtscher. Break-junctions for investigating transport at the molecular scale. *Journal of Physics: Condensed Matter*, 26(47):474201–, 2014.
- [8] Agrait N, Levy Yeyati A, and van Ruitenbeek J M. Quantum properties of atomic-sized conductors. *Physics Reports*, 377(23):81 – 279, 2003.
- [9] J. Ulrich, D. Esrail, W. Pontius, L. Venkataraman, D. Millar, and L. H. Doerr. Variability of conductance in molecular junctions. *J. Phys. Chem. B*, 110(6):2462–2466, February 2006.
- [10] Bingqian Xu and Nongjian J. Tao. Measurement of single-molecule resistance by repeated formation of molecular junctions. *Science*, 301(5637):1221–1223, August 2003.
- [11] Evan Evans. Probing the relation between force lifetime and chemistry in single molecular bonds. *Annu. Rev. Biophys. Biomol. Struct.*, 30(1):105–, June 2001.
- [12] M. Tsutsui, K. Shoji, M. Taniguchi, and T. Kawai. Formation and self-breaking mechanism of stable atom-sized junctions. *Nano Letters*, 8(1):345–349, 2008.
- [13] M. Alwan, N. Candoni, Ph Dumas, and H.R. Klein. Statistical evidence of strain induced breaking of metallic point contacts. *The European Physical Journal B*, 86(6), 2013.
- [14] M. Teresa Gonzalez, Jan Brunner, Roman Huber, Songmei Wu, Christian Schönenberger, and Michel Calame. Conductance values of alkanedithiol molecular junctions. *New Journal of Physics*, 10(6):065018–, 2008.
- [15] Yong-Hoon Kim, Hu Sung Kim, Juho Lee, Makusu Tsutsui, and Tomoji Kawai. Stretching-induced conductance variations as fingerprints of contact configurations in single-molecule junctions. *J. Am. Chem. Soc.*, pages –, May 2017.
- [16] M. T. Gonzalez, S. Wu, R. Huber, S. J. vanderMolen, C. Schönenberger, and M. Calame. Electrical conductance of molecular junctions by a robust statistical analysis. *Nano Lett.*, 6(10):2238–2242, October 2006.
- [17] Robert Quan, Christopher S. Pitler, Mark A. Ratner, and Matthew G. Reuter. Quantitative interpretations of break junction conductance histograms in molecular electron transport. *ACS Nano*, 9(7):7704–7713, 2015. PMID: 26168212.
- [18] Ben H. Wu, Jeffrey A. Ivie, Tyler K. Johnson, and Oliver L. A. Monti. Uncovering hierarchical data structure in single molecule transport. *The Journal of Chemical Physics*, 146(9):092321, 2017.
- [19] W. Haiss, R. J. Nichols, H. van Zalinge, S. J. Higgins, D. Bethell, and D. J. Schiffrin. Measurement of single molecule conductivity using the spontaneous formation wires. *Phys. Chem. Chem. Phys.*, 6(17):4330–4337, 2004.

- [20] Wolfgang Haiss, Harm van Zalinge, Donald Bethell, Jens Ulstrup, David J. Schiffrin, and Richard J. Nichols. Thermal gating of the single molecule conductance of alkanedithiols. *Faraday Discuss.*, 131:253–264, 2006.
- [21] V. Krachmalnicoff, E. Castanié, Y. De Wilde, and R. Carminati. Fluctuations of the local density of states probe localized surface plasmons on disordered metal films. *Phys. Rev. Lett.*, 105(18):183901–, October 2010.
- [22] T. Malinowski, H. R. Klein, M. Iazykov, and Ph. Dumas. Infrared light emission from nano hot electron gas created in atomic point contacts. *EPL*, 114(5):–, 2016.
- [23] J N Armstrong, R M Schaub, S Z Hua, and H D Chopra. Channel saturation and conductance quantization in single-atom gold constrictions. *Phys. Rev. B*, 82(19):195416, Nov 2010.
- [24] Brunner J, Gonzalez M T, Schönenberger C, and Michel Calame. Random telegraph signals in molecular junctions. *Journal of Physics: Condensed Matter*, 26(47):474202, 2014.
- [25] John Moreland and J. W. Ekin. Electron tunneling experiments using nb-sn “break” junctions. *Journal of Applied Physics*, 58(10):3888–3895, 1985.
- [26] U. Durig, L. Novotny, B. Michel, and A. Stalder. Logarithmic current-to-voltage converter for local probe microscopy. *Rev. Sci. Instrum.*, 68(10):3814–3816, October 1997.
- [27] David P. Doane. Aesthetic frequency classifications. *The American Statistician*, 30(4):181–183, November 1976.
- [28] J. W. Lynn, H. G. Smith, and R. M. Nicklow. Lattice dynamics of gold. *Phys. Rev. B*, 8(8):3493–3499, Oct 1973.
- [29] D. Vuillaume. Molecular-scale electronics. *Comptes Rendus Physique*, 9(1):78–94, 2008.
- [30] H. Liu, N. Wang, J. Zhao, Y. Guo, X. Yin, F. Boey and H. Zhang. Dependent Conductance of Molecular Wires and Contact Resistance in Metal/Molecule/Metal Junctions. *ChemPhysChem*, 9(10):1416–1424, 2008.
- [31] K.P.C Vollhardt. *Organic chemistry*. W.H. Freeman, New York, 1987.
- [32] Evangelina Pensa, Emiliano Cortes, Gaston Corthey, Pilar Carro, Carolina Vericat, Mariano H. Fonticelli, Guillermo Benitez, Aldo A. Rubert, and Roberto C. Salvarezza. The chemistry of the sulfur-gold interface: In search of a unified model. *Acc. Chem. Res.*, 45(8):1183–1192, August 2012.
- [33] Chen Li, Ilya Pobelov, Thomas Wandlowski, Alexei Bagrets, Andreas Arnold, and Ferdinand Evers. Charge transport in single au — alkanedithiol — au junctions: Coordination geometries and conformational degrees of freedom. *J. Am. Chem. Soc.*, 130(1):318–326, January 2008.
- [34] Frank Schreiber. Structure and growth of self-assembling monolayers. *Progress in Surface Science*, 65(5):151–257, 2000.

- [35] ZhengMing Wu, SongMei Wu, S. Oberholzer, M. Steinacher, M. Calame, and C. Schenberger. Scaling of $1/f$ noise in tunable break junctions. *Phys. Rev. B*, 78(23):235421–, December 2008.